

ORIGINAL ARTICLE

Sustainable and Green Zinc Oxide Nanoparticle Synthesis from Zingiber Officinale as a Wound Healing Accelerator

Zainab A. Najim*, Nasir A. Almansour, Hisham F. Mohammad

Department of Biology, College of Science, University of Basrah

ABSTRACT

Key words:

ZnO Nanoparticles, hydrogel, wound dressing, carbomer 940, Zingiber officinale Rosco

***Corresponding Author:**

Zainab A. Najim
Department of Biology,
College of Science, University
of Basrah
zainabmoha2025@gmail.com

Background: Zinc oxide nanoparticles are believed to be very useful in combating infections. Low toxicity, increased skin penetration of the relevant molecules, and protection against harmful germs are top priorities for optimal application in wounds. **Objective:** The aim of this work is the green-based synthesis of Zinc oxide nanoparticles from ginger and the characterisation of the resulting nanoparticles. **Methodology:** In this study we examined the effect of Zinc oxide nanoparticles on the healing process and accelerated wound healing in 12 strains of Balb/c mice. The mice were divided into four groups: two control groups, consisting of a group that received no treatment and a carbomer group, and two groups, one of which received the wound antibiotic Mebo and the other received the hybrid antagonist (ZnO+Carbomer940). On days 0, 2, 4, and 6, tissue contraction and wound size were evaluated. **Results:** The results showed that the hybrid antagonist (ZnO+Carbomer940) increased the wound closure and healing rate by 56.9%. In addition, the histological parameters, such as re-epithelialisation, accelerated hair follicle growth, and collagen layer regeneration were distinct and obvious. The study revealed no potential damage or infection. **Conclusion:** Compared with MEBO ointment and other control groups ZnO nanoparticles loaded with Carbomer940 hydrogel showed the ability to accelerate wound repair and hair growth within six days.

INTRODUCTION

Many comprehensive research studies have been conducted on many nanomaterials over the past years, but in our current era they are growing and flourishing and the use of nanotechnology which is considered an emerging and safe science is the focus of researchers to manufacture materials and metal particles on a nanoscale between 1-100 nanometres, which are environmentally degradable and low-cost. The green approach is used to replace old expensive methods such as physical and chemical methods known by their toxicity¹. The green approach is considered one of the best environmentally friendly, inexpensive, and safe methods. It is characterised by the manufacture of stronger metal nanoparticles that are coated with protein and have better dispersion and are unchangeable and can be included in many biological applications, including medical treatments².

Hybrid antagonist that includes nano Zinc oxide and carbomer 940 are among the treatments that can be included in biological applications such as wound healing, and the Carbomer 940 is commonly called Carbopol and is a high-molecular-weight synthetic polymer that is primarily used as a thickening agent in pharmaceutical and cosmetic formulations. When combined with nano Zinc oxide, it produces an excellent formulation that is showing progress in the

field of biomedical applications, especially in wound healing and as an antibacterial agent, because it has the ability to improve the stability and delivery of bioactive components such as ZnO³ and enhance the interaction between the two components and provide a sustained release of ZnO (NPs) while providing a protective barrier and an effective soothing of the skin^{3,4}.

The effect of ZnO made from ginger extracts, in particular, shows significant antimicrobial activity and is suitable for inclusion in various medical applications, such as the manufacture of some antibacterial agents and their potential in wound healing⁵. Ginger is a plant known for its increasing role in the green synthesis of metal particles, especially nano Zinc oxide, as this formulation exploits the natural properties of ginger extracts, providing an environmentally friendly alternative. Instead of traditional toxic chemical methods contribute to the synthesis of Zinc oxide nanoparticles, such as flavonoids and polyphenols where Zn²⁺ is reduced to its initial state, leading to the formation of Zinc oxide nanoparticles⁶⁻⁸ and Zinc oxide nanoparticles generated from ginger extracts, in particular, are often biologically compatible, making them suitable for inclusion in medical and biological applications and environmental restoration as well⁹⁻⁵. The wound is a complex and dynamic process as it requires a sequential understanding and management that leads to the healing process.

To fully evaluate wounds, experimental wounds can be performed on the skin of animals of a specific size and a specific uniform shape using punch biopsy to monitor the spontaneous shrinkage and understand the properties of the material to form the skin¹⁰⁻¹². Any damage to the integrity of body tissues such as skin, mucous membranes, or organs, is referred to as a wound in medical terminology. Many external sources, such as trauma from accidents, surgical procedures, or other violent actions such as mechanical and thermal forces, can cause this damage¹³.

Therefore, this study aims to generate Zinc oxide nanoparticles by green methods from ginger extract, followed by characterisation of the resulting metal particles using XRD, EF-SEM, TEM, UV-Vis, FTIR, and Zeta spectroscopy, and morphological evaluation and histological tests to demonstrate the effect and acceleration of the hybrid antimicrobial on the wound healing process.

METHODOLOGY

Preparation of Zinc oxide nanoparticles

The method according to (Hursima Izgis *et al.*)⁶ was followed in preparing the aqueous extract of ginger from the ginger plant and the following concentrations were prepared from it (0.5, 0.25, 0.125, 0.0625%). 400 ml of 0.01 M zinc acetate dihydrate were prepared using deionized water. The prepared concentrations of ginger extract were added separately to the zinc acetate dihydrate solution slowly under magnetic stirring, and to obtain a pH = 12, 1.0 M NaOH was used. After reaching the desired pH, the mixture was stirred for three hours until a white precipitate was formed. This mixture was centrifuged at a speed of $10,000 \times 10$ min. The upper precipitate was discarded, and the ZnO nanoparticle powder was washed with deionized water and dried at 100°C overnight. The resulting powder was collected and weighed.

Characterization of Synthesized ZnO NPs

All tests were conducted at Sharif University of Technology (SUT)\Iran. The morphological features of the synthesised ZnO nanoparticles using the collected plants were observed by field emission scanning electron microscope (FE-SEM), then transmission electron microscopy (TEM) was used to analyse the shape, size, and distribution of ZnO nanoparticles. In addition to UV-Vis spectroscopy analysis, UV-Vis spectroscopy was performed¹⁴.

To characterize the structural properties of the nanoparticles by determining the absorption, the UV-Vis spectra range was taken between 0.1100-255.0 nm where the formation of the characteristic plasmon resonance band was observed depending on the particle size and shape and the UV-Vis absorption of ZnO nanoparticles shows the characteristic plasmon resonance peak range between 300 and 400 nm. Fourier

transform infrared spectroscopy (FTIR) was performed to determine the presence of functional groups in the synthesized ZnO nanoparticles, which facilitates the biosynthesis process¹⁵.

As for the X-ray diffraction results, X'pert Pro X-ray diffraction (XRD) was used, and the powder diffraction pattern of the synthesized nanoparticles was recorded. The zeta potential method was used to evaluate the stability of ZnO nanoparticles using a zeta potential analyser from Malvern Instruments Ltd., and the nanoparticles were measured between -200 and +200 at 25.2 °C¹⁶.

Preparation of carbomer and Zinc oxide nanoparticles (CNPs) for topical use

The hybrid antagonist Zinc Oxide nanoparticles (ZnO NPs) and carbomer 940 (CNPs) were prepared according to the method of Ismail *et al.*³ with slight modification (1 gm) of carbomer 940 was dissolved in 300 ml of deionized water twice, followed by the addition 100 µg/ml of freshly washed ZnO nanoparticles to ensure a thick consistency. Since carbomer 940 is acidic in nature, the solution should be neutral by following this step. After that, the mixture was mixed with a small-volume electric mixer for 20 min and then 50 ml of Triethylamine (TEA) were added as a neutralizing agent (raising the pH to 7) drop wise. Continuous stirring until the formation of white ZnO gel occurred, Carbomer 940 became thick when the pH approached neutrality.

Experimental animal

This step was conducted at the University of Basrah, College of Science/Iraq/Department of Biology. The experimental animals were kept in the animal house of the Department of Life Sciences. Twelve healthy adult males of the same strain of BALB/c mice were tested¹⁷. Their ages ranged from 4-6 months, and their weights ranged from 30-40 grams. All mice were housed under standard laboratory conditions with a 12-hour light/12-hour dark cycle and a temperature of 18-22°C. The animals were maintained with adequate nutrition and access to water with ventilation in the housing area of the animal house where the study was conducted.

Wound Evaluation

This study was conducted to investigate the potential of the hybrid antagonist (ZnO+Carbomer940) to accelerate wound healing in mice. A total of 12 mice with shoulder biopsy wounds were included in the study. The mice were divided into four groups, A, B, C, and D, each consisting of 3 mice. The mice in group A were treated without treatment, while those in group B were treated with Carbomer 940 hydrogel, mice in group C were treated with Mebo cream, and the last group D was treated with the treatment of hybrid antagonist (ZNO+Carbomer 940).

Wounding criteria

Rats were anaesthetised with a mixture of 10% xylazine and 2% ketamine and the anaesthetic was

injected intraperitoneally using 0.5 ml insulin needles, where 0.1 ml of the anaesthetic mixture was injected for every 10 g of rat weight. The wound area was prepared by removing the hair between the shoulders down to the pelvis using an electric shaver and a small amount of depilatory agent. A disposable biopsy drill was used to create excisional wounds after anaesthesia, and 8 mm of skin were removed. Rats were kept in regular individual

polypropylene cages. They were distributed according to (Table 1). The newly created wounds were treated by adding the hybrid antiserum and applying the material to the wound surface and then distributing it with a cotton swab every 24 hours. The study parameters were microscopic evaluation and wound contraction size (mm) on days 0, 2, 4, and 6 using a calliper.

Table 1: Experimental design of the animals

Sr. No	Groups	No. of Animals	Treatment Protocol	Application	Frequency
1.	Group A	3Mice	without treatment	Direct application with Cotton Swab	After 24 hours
2.	Group B	3Mice	carbomer 940	Direct application with Cotton Swab	After 24 hours
3.	Group C	3Mice	Mebo cream	Direct application with Cotton Swab	After 24 hours
4.	Group D	3Mice	hybrid antagonist (ZnO+Carbomer940)	Direct application with Cotton Swab	After 24 hours

Wound Contraction Rate (%)

Wound healing was evaluated by measuring the wound contraction rate at days 0, 2, 4, and 6. It was calculated by the following formula:

$$\% \text{ Wound contraction} = \frac{\text{initial wound size} - \text{specific day wound size}}{\text{initial wound size}} * 100$$

RESULTS

Characterization of ZnO nanoparticles (NPS)

The characterization results as shown in (Fig. 1-3) indicate that the ZnO nanoparticles synthesised from ginger extract possess distinct morphological and chemical properties. Field emission scanning electron microscopy (FE-SEM) revealed a cauliflower-like morphology with aggregated spherical dimensions and sizes up to 18.21 nm. This shape can enhance certain functions, such as drug delivery or stimulation, by providing a larger surface area. Transmission electron microscopy (TEM) analysis confirmed the crucial

insights into the structure of ZnO nanoparticles. This analysis allowed high-resolution imaging of ZnO nanoparticles. Their shape and size were evaluated at the nanoscale and were found to be spherical and consistent with each other. In addition, UV-Vis spectroscopy showed a peak at 366 nm, indicating the successful biosynthesis of ZnO nanoparticles through sustainable green synthesis. Fourier transform infrared spectroscopy (FTIR) analysis was determined. The characteristic values at wave numbers (690.52 and 925.83) cm⁻¹ were negative, indicating the presence of a Zn-O bond. XRD analysis showed that the nanoparticles had three characteristic peaks, and the amplitude of the diffraction peak line is an indication that the synthesised material belongs to the group of ZnO nanoparticles, and the peaks were 20 = 31.7183, 34.4588, 47.5488, and 36.251, while the zeta potential (ζ) analysis indicated that the value of -11.2 mV is considered to have a certain degree of stability.

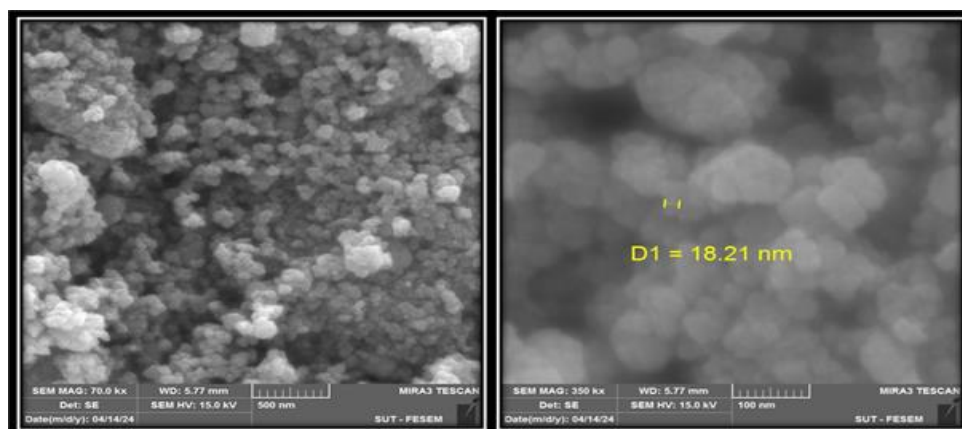


Fig. 1: FE-SEM image of ZnO nanoparticles

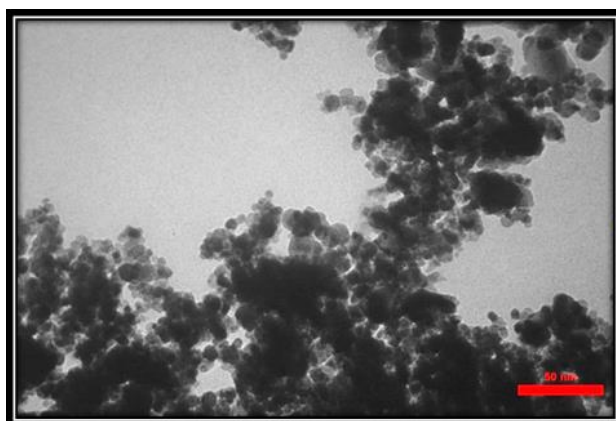


Fig. 2: Transmission electron microscope image of ZnO NPs

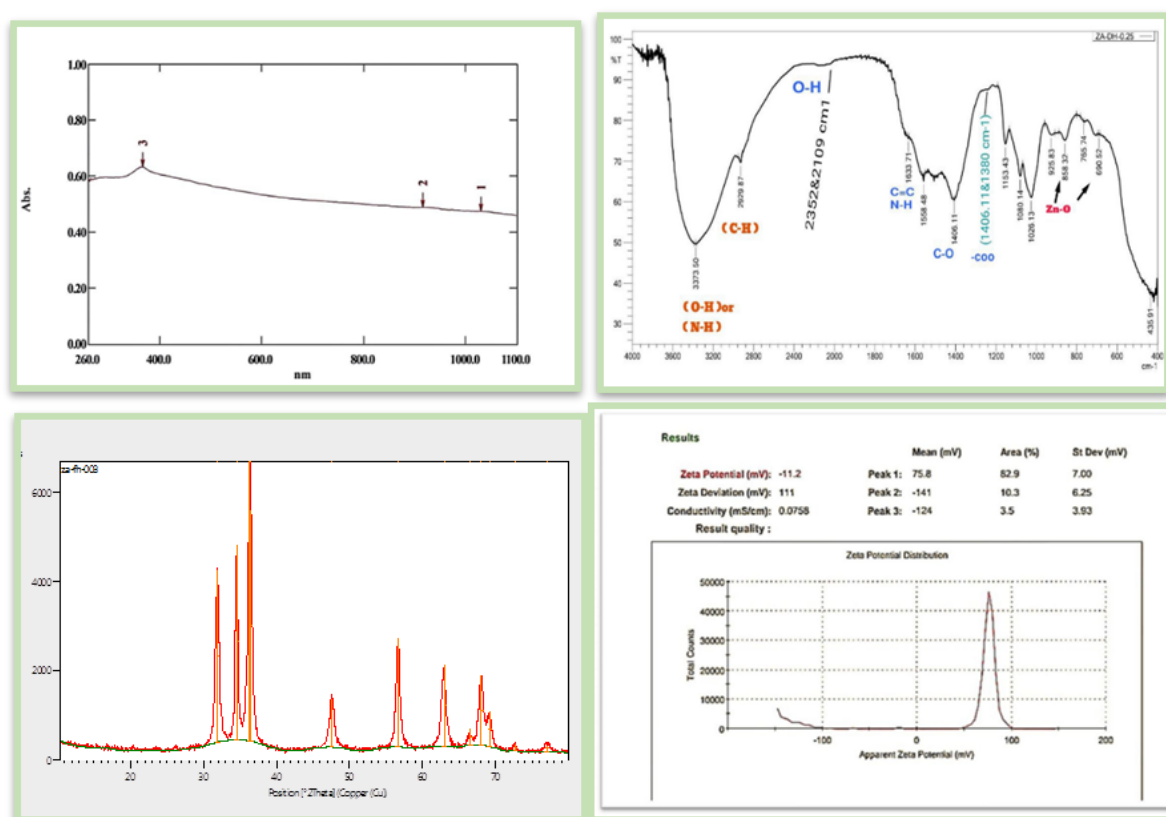


Fig. 3: UV-Vis spectra, FTIR spectra, XRD pattern and Zeta Potentials of ZnO nanoparticles

Wound Evaluation Results

The following parameters were evaluated:

Evaluation Criteria

Wound Size (mm)

As shown in table 2. The treatment protocol was applied to the respective groups from day 0 to day 6. Wound size and contraction were measured in each mouse by Vernier callipers, and readings were taken on days 0, 2, 4, and 6. The collected data regarding wound size and contraction were analysed by one-way analysis of variance using Minitab@22.2.1 Statistical Software,

2024, and the statistical analysis showed that the data were significant at $p \leq 0.05$.

Wound size of BALB/c Mouse in group (A) (control group)

In group (A) 3 mice with puncture wounds were left untreated. They were monitored until day 6. The average wound size of mice on day (0) was 8.00 ± 0.00 , while on day (2) it was 7.083 ± 0.62 , while on day (4) it was 6.050 ± 0.27 and on day (6) the wound size was found to be 5.700 ± 0.39 .

Wound size of BALB/c Mouse in group (B) (Carbomer 940 hydrogel)

In group (B), 3 mice with puncture wounds of 8 mm size were treated with Carbomer 940, and the average wound size in mice on day (0) was 8.00±0.00; on day (2), it was 6.333±0.28, and up to day 4, it was 6.100±0.54, while on day (6), it became 5.250±0.00, 8, out of a total of 6 wounds. Out of a total of 3 cases, little wound healing with irritation at the wound site was observed for the three replicate mice.

Wound size of BALB/c Mouse in (group C) Mebo Cream

Three mice with puncture wounds of 8 mm diameter were treated with Mebo cream, and the average wound size of the mice on day (0) was 8.00±0.00, on day (2) it

was 8.000±0.00, and on day (4) it was 7.800±0.34, while on day (6) it became 6.633±0.58, and it was noted that there was complete irritation with the appearance of a clot above the skin surface.

Wound size of BALB/c Mouse in Group D hybrid antagonist (ZnO+Carbomer940)

Three mice with 8 mm puncture wounds were treated with hybrid antagonists -(ZnO+Carbomer940) and the average wound size of the mice on day (0) was 8.00±0.00, on day (2) it was 5.583±0.38 and up to day (4) it was 4.783±0.41 while on day (6) it became 3.217±1.52, from a total of 3 replicates the wound healing speed was observed within six days of wound formation with faster hair growth compared to the other three treatments.

Table 2: Wound area reduction rate at each time point (±standard deviation)

Treatment	Wound healing rate in days means (mm) & St. Dev			
	0	2	4	6
G1A	8.00±0.00	7.083±0.62	6.050±0.27	5.700±0.39
G2B	8.00±0.00	6.333±0.28	6.100±0.54	5.250±0.00
G3C	8.00±0.00	8.000±0.00	7.800±0.34	6.633±0.58
G4D	8.00±0.00	5.583±0.38	4.783±0.41	3.217±1.52
	Lsd=0.000	Lsd=0.913	Lsd=0.940	Lsd=2.05

Wound Contraction Rate (%), Graphical representation of wound contraction rate in all groups

As shown in table 3 and (Fig. 4), the wound size in groups (A), (B), (C) and (D) was similar on day zero. In the graph, the dark blue colour indicates the size of the wound contraction in group (A) (the control group without treatment); the red colour indicates the size of the wound contraction in group (B) (Carbomer 940), which reached 34.3% and represents the highest healing rate compared to groups (A) and (C), while the green colour indicates group (C). It represents the percentage of wound contraction (for treatment with Mebo cream), and it was noted that it was the lowest percentage among the four groups, which reached 17.0%, and the sky-blue colour showed the highest percentage, which is 59.7% in terms of complete wound healing, and the hybrid antagonist (ZnO + Carbomer 940) went to group (D). From the graph, it was clear that the wounds treated with Zinc oxide nanoparticles, group D, contracted faster and healed more effectively compared to the wounds treated without treatment, carbomer 940, and Mebo cream A, B, C, respectively.

Table 3: wound contraction rate (%)

Treatment	Wound healing contraction rate (%) in days			
	0	2	4	6
G1A	0%	11.4%	24.3%	28.7%
G2B	0%	20.8%	23.75%	34.3%
G3C	0%	0%	25%	17.0%
G4D	0%	30.2%	40.2%	59.7%

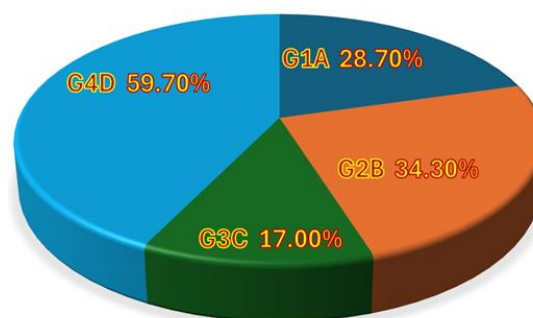


Fig. 4: Pie chart showing wound healing shrinkage rate (%) at the sixth day for each treatment.

Wound healing activity

The wound results as shown in (Figure 5) from day 0 to day 4 showed signs of contraction that were not completely clear, with slight contraction of the wound circumference and noticeable appearance of irritation and blood clots above the fresh wounds from day 2 to day 6. This was the case for group (A) which was represented by the protocol without treatment. The wounds were not yet completely healed. As for group (B) which followed the protocol of treatment with the antibiotic Carbomer 940, it showed clear signs of wound healing slightly higher than groups (A) and (B) with irritation on the skin surface for the three versions of the wounds, but slight contraction of the wound edges was observed starting from day 2, and the appearance of a blood clot and a clear upper protrusion of the blood clot above the level of the newly formed wound on day 6. As for the results of the group that followed the Mebo cream protocol (group C), it was noted that the healing speed was less than groups A and

B, and irregularity in the shape of the wound was observed due to irritation, redness and bleeding, followed by a sudden, almost complete closure on the sixth day, which was striking, and the three wounds were on their way to slow healing, while the wound bed was completely covered with a thin layer of congealed blood and clear irritation starting from day (2). As for the results of group D, which used a hybrid anti-treatment strategy that included carbomer 940 and nano zinc oxide, they were excellent in terms of the speed of complete wound healing within (6) days, as it was characterized by the fastest healing rate and the absence of irritation or skin bleeding on the wound surface starting from the first day, which is considered the best result when compared to the three treatments (A, B, C), and the speed of closure was faster than the usual period of 7 to 14 days, and hair growth was observed at a significant rate; the wound bed was completely covered with new skin cells, and no visible scars were formed.

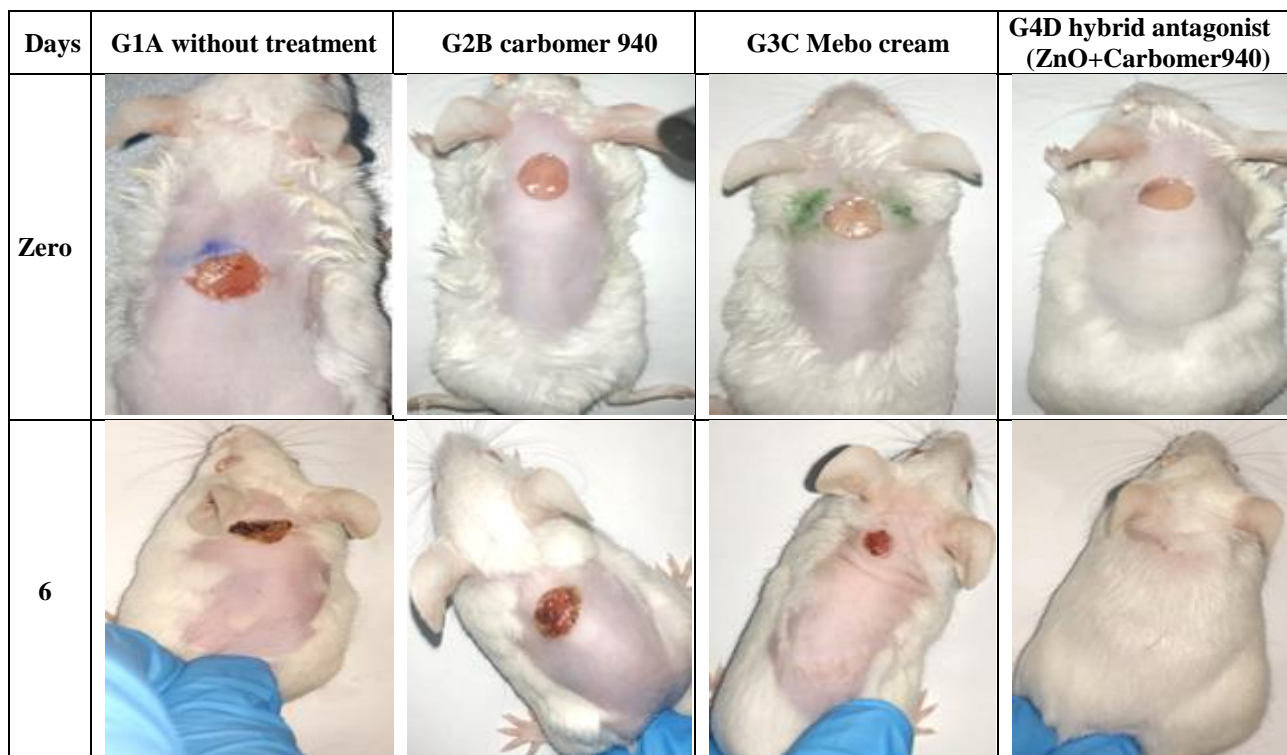


Fig. 5: Stages of wound healing in BALB/c Mouse skin using hybrid antagonist (ZnO+Carbomer940)

DISCUSSION

The characterisation results, as shown in (Fig. 1-6), FE-SEM and TEM indicate that ZnO NPs were successfully synthesised, as their shape and size were evaluated at the nanoscale and found to be spherical and consistent with each other. These results were relevant to other reports¹⁸⁻¹⁹, as well as UV-visible spectroscopy, where the results were similar to other studies²⁰⁻²¹, on

the synthesis of ZnO nanoparticles using parthenium leaf extract and citric acid, which reached 374 nm, while the Fourier transform infrared spectroscopy (FTIR) analysis had distinct peaks indicating the presence of Zn-O bond. These results are consistent with similar studies²²⁻²³. X-ray diffraction analysis showed that the nanoparticles had three distinct peaks, and the peak results showed a fairly close agreement with other results²⁴⁻²⁵. While the zeta potential (ζ)

analysis indicated a result with some degree of stability, it is at the lower end of the scale, and the results of the present study are consistent with what was reported for the zeta potential test of ZnO nanoparticles that if the value of (ζ) is greater than +30 or less than -30, the suspension is considered stable, and the higher the value, the more stable the formulations²⁶⁻²⁷.

The wound healing activity results as shown in (Tables 2 and 3) and (Fig. 5) of ZnO nanoparticles were verified on the wound area formed on the back of BALB/c mice strain for groups (group 1A, group 2B, group 3C, group 4D) over six days after excision wounds were created. It is worth noting that the hybrid treatment group 4D, at a concentration of 100 $\mu\text{g/ml}$, showed wound closure rate of up to 59.7%. After six days, it was observed that the hair growth rate exceeded that of the rest of the treatments (group 1A, group 2B, group 3C).

The results of our study were closely related to another study which reported that wounds in zebrafish closed by 54% at a concentration of 40 ($\mu\text{g/ml}$) after seven days of wounding, and the closure increased significantly to 62% at a concentration of 80 ($\mu\text{g/ml}$) when compared to the control groups²⁸. The results of our study confirmed the potential efficacy of ZnO (NPs) in promoting faster wound healing, indicating that result is promising for further exploration in wound healing applications. Faster wound healing when products containing ZnO (NPs) were applied is attributed to several properties including that ZnO (NPs) applied to wounds can increase keratinocyte proliferation, migration and promote epithelialization which help in faster wound closure by promoting epithelial cell growth. Zinc oxide particles play an important role in collagen synthesis, which is vital for tissue remodelling activity during the healing phase, contributing to faster healing by ensuring rapid closure of the wound surface²⁹.

The focus in wound therapy remains on testing biocompatible compounds that exhibit biocompatibility which accelerates wound closure and the healing and regeneration of damaged tissues as quickly as possible. The effectiveness of the hybrid antiseptic (ZnO+Carbomer940) is due to the fact that it contains zinc oxide nanoparticles in addition to carbomer 940, which facilitates the access of these nanoparticles to the damaged tissues and promotes the stages of wound healing. When combined together, they will create a valuable treatment that accelerates complete healing, as carbomer primarily provides a moist environment while promoting blood flow to the injured tissues and modulating inflammation. Zinc oxide nanoparticles contribute to antimicrobial protection, stimulate cellular activity, and maintain adjuvant moisture, which increases the effectiveness and excellent result in wound healing^{30,31}.

CONCLUSION

Our study highlights the multifaceted therapeutic potential of sustainable ZnO nanoparticles and the ability of the hybrid antagonist (ZnO+Carbomer 940) to accelerate wound healing. The synergistic combination of the hybrid antagonist provided a promising basis for rapid wound healing in record time. In addition to the well-known wound moisturizing benefits of the hybrid antagonist (ZnO+Carbomer940), the green synthesis of ZnO nanoparticles resulted in low-toxic protein-coated particles, contributing to the success of the experiment in a sustainable and safe manner. The hybrid antagonist (ZnO+Carbomer940) therapy presented promising potential in keratinocyte migration, epithelialization, accelerated healing, and enhanced tissue repair.

Ethical approval

All procedures performed in the studies involving BALB/c mouse were in accordance with the ethical standards of the Institutional Research Committee of the University of Basrah - College of Science.

Funding

This work is self-funding.

Conflict of interest

The authors state no conflict of interest for the research, authorship, and/or publication of this article.

REFERENCES

1. Sahu MK, Yadav R, Tiwari SP. Recent advances in nanotechnology. *Inter J of Nanomate, Nanotechno and Nanomed.* 2023;9(2):15–23.
2. Putta S, Sharma RK, Khandelwal P. Metal Nanoparticles: Synthesis, Characterization, and Biomedical Applications. *Nanomat.* 2023;85-102.
3. Ismail SH, Hamdy A, Ismail TA, Mahboub HH, Mahmoud WH, Daoush WM. Synthesis and Characterization of Antibacterial Carbopol/ZnO Hybrid Nanoparticles Gel. *Cryst.* 2021;11(9):1092.
4. Hassan RRA, Hassan HM, Mohamed YA, Ismail MEM, Farid Y, Mohamed H, et al. ZnO, TiO₂ and Fe₃O₄/Carbopol hybrid nanogels for the cleaner process of paper manuscripts from dust stains and soil remains. *Heri Sci.* 2023;11(1):1-26.
5. Shakir L, Janakiraman AK, Sharmanee Thiagarajah, Baskaran Gunasekaran, Khanna K, Kumar A, et al. Green synthesis of ginger-encapsulated zinc oxide nanoparticles: Unveiling their characterization and selective cytotoxicity on MDA-MB 231 breast cancer cells. *J of Adv Pharma Techno amp Res.* 2023;14(4):325–331.
6. Omran IM, Hassan KS, AlMansour NAA. Evaluation of plants extracts on mortality and development of Saw-toothed Grain beetle, *Oryzaephilus surinamensis* L. (Coleoptera: Silivianidae). *Ind J Of Ecol.* 2021;48(15):160-164.

7. ICC ICC, hilo duoa H, al-garawi zahraa s, ismail hmad h. Green synthesis of ZnO NPs using ginger extract and assessment of their antioxidant activity. *Egy J of Chem.* 2022;66(5):111–117.
8. Aliannezhadi M, Seyede Zahra Mirsanaee, Jamali M, Fatemeh Shariatmadar Tehrani. The physical properties and photocatalytic activities of green synthesized ZnO nanostructures using different ginger extract concentrations. *Sci Rep.* 2024;14(1):2035-2048.
9. Raj LFA, Jayalakshmy E. Biosynthesis and Characterization of Zinc Oxide Nanoparticles Using Root Extract of Zingiber Officinale. *Orie J of Chem.* 2015;31(1):51-56.
10. Guo S, DiPietro LA. Factors Affecting Wound Healing. *J of Den Res.* 2020;89(3):219–229.
11. Eming SA, Martin P, Tomic-Canic M. Wound repair and regeneration: Mechanisms, signaling, and translation. *Sci Trans Med.* 2014;6(265):1-16
12. Labib A, Winters R. *Complex Wound Management.* Publishing; 2023. Available from: <http://www.ncbi.nlm.nih.gov/books/NBK576385/>
13. Kujath P, Michelsen A. Wounds-From Physiology to Wound Dressing. *Deuts Aertz Inter.* 2008;105(13):239-248.
14. Jawad EK., Jaffer KS, Mohammad HF. Preparation of Fortified Edible Gelatin Films Nanoscale Magnesium Oxide and Study of Its Mechanical and Antibacterial Effectiveness. *Univer of Thi-Qar J Of Med.* 2024;28(2): 361-371.
15. Khaleefa RS, Al-Hejuje MM, Mohammad HF. A novel electrochemical assay based biological synthesis nanoparticles for some hydrocarbons using single-stranded DNA-binding aptamer. *Ann of For Res.* 2022;65(1): 8132-8143.
16. Marsalek R. Particle Size and Zeta Potential of ZnO. *APCBEE Proce.* 2014;9:13–7.
17. Nakamura H. BALB/c Mouse. *Brenner's Encyclopedia of Genetics.* 2nd. Acade Press. 2013;290–292. eBook ISBN: 9780080961569
18. Raha S, Ahmaruzzaman M. ZnO nanostructured materials and their potential applications: Progress, challenges and perspectives. *Nanosc Advan.* 2022;4(8):1868–1925.
19. Albarakaty FM, Alzaban MI, Alharbi NK, Bagrwan FS, Abd El-Aziz ARM, Mahmoud MA. Zinc oxide Nanoparticles, Biosynthesis, characterization and their potent photocatalytic degradation, and antioxidant activities. *J of King Saud Univer-Sci.* 2023; 35(1):102434.
20. Rajiv P, Rajeshwari S, Venckatesh R. Bio-Fabrication of zinc oxide nanoparticles using leaf extract of Parthenium hysterophorus L. and its size-dependent antifungal activity against plant fungal pathogens. *Spectrochi Acta Part A: Mole and Biomole Spectro.* 2013; 112: 384–387.
21. Taranath T, Patil B. Limonia acidissima L. leaf mediated synthesis of zinc oxide nanoparticles: A potent tool against Mycobacterium tuberculosis. *Inter J of Mycobacterio.* 2016; 5(2):197-204.
22. Fakhari S, Jamzad M, Kabiri Fard H. Green synthesis of zinc oxide nanoparticles: A comparison. *Green Chem Lett and Rev.* 2019; 12(1): 19–24.
23. Motazedi R, Rahaiee S, Zare M. Efficient biogenesis of ZnO nanoparticles using extracellular extract of Saccharomyces cerevisiae: Evaluation of photocatalytic, cytotoxic and other biological activities. *Bioorgan Chem.* 2020; 101: 103998.
24. Barrak H, Saied T, Chevallier P, Laroche G, M'nif A, Hamzaoui AH. Synthesis, characterization, and functionalization of ZnO nanoparticles by N-(trimethoxysilylpropyl) ethylenediamine triacetic acid (TMSEDTA): Investigation of the interactions between Phloroglucinol and ZnO@TMSEDTA. *Arab J of Chem.* 2019; 12(8): 4340–4347.
25. Basnet P, Samanta D, Chanu I, Mukherjee J, Chatterjee S. Assessment of synthesis approaches for tuning the photocatalytic property of ZnO nanoparticles. *SN App Sci.* 2019; 1:1-13.
26. Eskin A, Nurulloğlu Z. Open Access Effects of zinc oxide nanoparticles (ZnO NPs) on the biology of Galleria mellonella L. (Lepidoptera: Pyralidae). *The J of Bas and App Zoo.* 2022; 83: 54-66.
27. Krishnakumar V, Elansezhian R. Dispersion stability of zinc oxide nanoparticles in an electroless bath with various surfactants. *Mat Tod: Proce.* 2022; 51: 369–373.
28. Krishnakumar VR. Elansezhian. Dispersion stability of zinc oxide nanoparticles in an electroless bath with various surfactants. *Mat Tod: Proce.* 2022; 51:369-373.
29. Ågren M, Phothong N, Burian E, Mogensen M, Hædersdal M, Jorgensen L. Topical Zinc Oxide Assessed in Two Human Wound-healing Models. *Acta Derm Venereo.* 2021;101(5):712-714.
30. Chen CY, Yin H, Chen X, Chen TH, Liu HM, Rao SS, et al. Ångstrom-scale silver particle-embedded carbomer gel promotes wound healing by inhibiting bacterial colonization and inflammation. *Sci advan.* 2020;6(43):1-14.
31. Wang D, Jin J, Zhang C, Ruan C, qin Y, Li D, et al. Carbomer Hydrogel Composed of Cu₂O and Hematoporphyrin Monomethyl Ether Promotes the Healing of Infected Wounds. *ACS Omega.* 2024;9(4):4974-4985